JOURNAL OF GUIDANCE, CONTROL, AND DYNAMICS
Vol. 16, No. 5, September–October 1993

Full Envelope Multivariable Control Law Synthesis for a High-Performance Test Aircraft

Richard J. Adams, Andrew Sparks, and Siva S. Banda
Wright Laboratory, Wright-Patterson Air Force Base, Ohio 45433

A full envelope multivariable flight control system is developed for the Variable Stability In-Flight Simulator Test Aircraft (VISTA). Separate control laws are designed for the longitudinal and lateral directional axes. Output feedback controllers with integral error feedback are created using linear quadratic synthesis and simple linear transformations. Longitudinal stick inputs are used to generate an angle-of-attack command at low-dynamic pressure and a normal acceleration command at high-dynamic pressure. Lateral stick inputs are used to generate a stability axis roll rate command, and rudder pedal inputs are used to generate a sideslip command. Linear point designs are integrated into a gain schedule to create a full envelope nonlinear control system. Flying qualities are evaluated according to military standards and shown to be satisfactory for a wide operating envelope. Classical gain and phase margins and analysis of the structured singular value show robustness to be acceptable for a wide operating envelope.

Nomenclature

A_z = normal acceleration at c.g., g
J = performance index
n = load factor
p = body axis roll rate, rad/s
q = body axis pitch rate, rad/s
$\bar{q}$ = dynamic pressure, psf
r = body axis yaw rate, rad/s
T_R = roll time constant, s
T_S = spiral time constant, s
$T_{\theta 2}$ = pitch response time constant, s
u_{lat} = lateral input vector
u_{lon} = longitudinal input vector
V = velocity, ft/s
W_0 = vertical velocity, ft/s
x_{lat} = lateral state vector
x_{lon} = longitudinal state vector
y_{lon} = longitudinal output vector
z = performance variable
α = angle of attack, rad
β = sideslip angle, rad
δ_a = aileron deflection, rad
δ_{df} = asymmetric flap deflection, rad
δ_{dt} = asymmetric tail deflection, rad
δ_e = symmetric tail deflection, rad
δ_{pedal} = rudder pedal force, lbf

Richard J. Adams, Captain U.S. Air Force, received a B.S. degree in Engineering Sciences from the United States Air Force Academy in 1989 and an M.S. in Aeronautics and Astronautics from the University of Washington in 1990. He is currently a stability and control engineer in the Flight Dynamics Directorate at Wright Laboratory, Wright-Patterson Air Force Base. His research interests include high angle-of-attack stability and control and the application of multivariable control theory to realistic flight control design. He is a Member of AIAA.

Andrew Sparks graduated with a B.S. and an M.S. in Mechanical Engineering from Massachusetts Institute of Technology in 1986 and 1988, respectively. From February 1988 to August 1992 he worked as a Stability and Control Engineer in the Flight Controls Division of the Wright Laboratory. He is currently working on his Ph.D. at the University of Michigan in the Department of Aerospace Engineering. He is expected to return to the Wright Laboratory in 1995. His research interests include robust control theory and its application to aircraft. He is a Member of AIAA.

Siva S. Banda is an Aerospace Engineer at Wright Laboratory, Wright-Patterson Air Force Base, Ohio. His responsibilities include transitioning basic research results in the area of control theory to the aerospace industry. He has authored or coauthored more than 75 publications in the areas of multivariable control theory and application. He has received numerous awards from the U.S. Air Force for scientific achievement including the Air Force Chief of Staff award from the Pentagon. He has served as a member of the AIAA Guidance, Navigation, and Control Technical Committee, on the Board of Directors of the American Automatic Control Council, as Chairman of the AIAA Awards Committee, and as Associate Editor of the *Journal of Guidance, Control, and Dynamics*. He has been an Adjunct Associate Professor at Wright State University and at University of Dayton. He is a Fellow of Wright Laboratory and is an Associate Fellow of AIAA.

Received May 1, 1992; presented as Paper 92-4408 at the AIAA Guidance, Navigation, and Control Conference, Hilton Head, SC, Aug, 10–12, 1992; revision received Sept. 28, 1992; accepted for publication Nov. 22, 1992.

δ_r = rudder deflection, rad
δ_{stickp} = pitch stick force, lbf
δ_{stickr} = roll stick force, lbf
ζ_D = Dutch roll damping
ζ_{sp} = short period damping
$\dot{\mu}$ = stability axis roll rate, rad/s
τ_P = pitch prefilter time constant, s
τ_{ped} = pedal prefilter time constant, s
τ_R = roll prefilter time constant, s
τ_β = equivalent sideslip time delay, s
τ_θ = equivalent pitch time delay, s
τ_μ = equivalent roll time delay, s
ϕ = roll angle, rad
ω_D = Dutch roll frequency, rad/s
ω_{sp} = short period frequency, rad/s

Introduction

THE Variable Stability In-flight Simulator Test Aircraft (VISTA) program is ongoing in the Flight Dynamics Directorate of Wright Laboratory. The VISTA aircraft will be used to study new technology in the control of advanced configuration vehicles and advanced control concepts. The baseline aircraft being modified to create the VISTA is the F-16. Multiple control system capability gives the aircraft the ability to test advanced control systems in-flight while maintaining the ability to revert to its conventional systems in the event of difficulties. An extended angle-of-attack capability is desired to allow the VISTA F-16 to achieve maximum lift, thus giving it the ability to simulate the capabilities of more advanced high-performance aircraft.

The goal of in-house efforts for the VISTA F-16 in the Flight Dynamics Directorate's Control Dynamics Branch is to achieve good handling qualities and robustness over a wide operating envelope by using advanced control approaches to augment stability and performance. One approach being undertaken is to use multivariable control to synthesize new control laws for the VISTA F-16. This involves developing controllers for the existing operational envelope using multivariable synthesis techniques. The purpose of redesigning the control system for conventional flight is to gain experience with the aircraft's capabilities and limitations and to provide a baseline control structure for the transition to high angle-of-attack flight control.

In this paper, the results of the longitudinal and lateral directional control law design for the full conventional maneuvering envelope are presented. First, descriptions of the aircraft and the nonlinear model are given. Then, a list of design requirements from flying qualities and robustness specifications is presented. The linear models used for control system design are described next. Linear quadratic regulator (LQR) theory is reviewed, and the control law design process using LQR theory with integral action is shown. Linear and nonlinear elements are used to build the command shaping feedforward loops. The control gains at several design points are scheduled with dynamic pressure to form an implementable full envelope controller. Nonlinear time responses to pilot inputs are plotted to show performance. Finally, flying qualities and robustness analyses are performed and the results presented.

Design Goals

The performance requirements of interest are the flying qualities requirements in MIL-STD-1797.[1] These requirements give measures of whether the aircraft has acceptable response to pilot inputs. Several flying qualities requirements are based on low-order equivalent system approximations of the actual dynamics. The maximum allowable error in gain and phase between a high-order transfer function and a low-order equivalent system is specified as a function of frequency. These gain and phase bounds represent the range of dynamics that are considered unnoticeable to pilots.

Pitch axis control is the critical element in longitudinal flying qualities. Control of normal acceleration is the pilot's primary means of maneuvering. During missile delivery, the pilot directly controls pitch angle to put his target within the lethal radius of his weapons. In gunnery maneuvers, a pilot directly controls pitch to point the aircraft at his target. Pitch is also used indirectly to control flight path in situations such as holding a landing approach.

Aircraft flying qualities requirements for the pitch axis are given in terms of low-order equivalent systems that represent the pitch rate and normal load factor responses to pilot control force inputs.

$$\frac{q}{\delta_{stickp}} = \frac{K_q(s+1/T_{\theta 2})e^{-\tau_\theta s}}{s^2+2\zeta_{sp}\omega_{sp}s+\omega_{sp}^2}, \qquad \frac{A_z}{\delta_{stickp}} = \frac{K_{nz}e^{-\tau_\theta s}}{s^2+2\zeta_{sp}\omega_{sp}s+\omega_{sp}^2} \tag{1}$$

The military standard guidelines for control anticipation parameter (CAP), equivalent short period damping and frequency, equivalent pitch time delay, and $\omega_{sp}T_{\theta 2}$ are selected as the evaluation criteria for the longitudinal design. CAP is defined as

$$\text{CAP} = \omega_{sp}^2/(n_z/\alpha) \tag{2}$$

For category A flight phases, level I flying qualities[1] require that the CAP be between 0.28 and 3.60. The short period frequency must be greater than 1.0 rad/s, and the short period damping must be between 0.35 and 1.3. The equivalent time delay must be less than 0.10 s, and the product $\omega_{sp}T_{\theta 2}$ must be greater than 1.85.

The basic philosophy of the lateral flight control laws is to provide control of the stability axis roll rate and the sideslip angle. Control of stability axis roll rate rather than body axis roll rate reduces kinematic coupling during rolls at high angles of attack. At low angles of attack, body and stability axis roll rates are practically the same. Control of sideslip angle helps maneuvers to be coordinated and allows landing in a crosswind.

The low-order equivalent system used for lateral directional flying qualities analysis is the fourth-order transfer function from pilot stick force to roll rate. Since the objective is the control of stability axis roll rate, the transfer function used for the analysis is that from the lateral stick to stability axis roll rate.

$$\frac{\dot{\mu}}{\delta_{stickr}} = \frac{K_\mu(s^2+2\zeta_\mu\omega_\mu s+\omega_\mu^2)e^{-\tau_\mu s}}{(s+1/T_R)(s+1/T_S)(s^2+2\zeta_D\omega_D s+\omega_D^2)} \tag{3}$$

To meet level I flying qualities,[1] the equivalent Dutch roll frequency must be higher than 1 rad/s and the equivalent Dutch roll damping ratio must be larger than 0.19. The equivalent roll mode time constant must be less than 1.0 s. The equivalent spiral mode must be stable or have a time to double amplitude of greater than 12 s after a perturbation in roll angle. Finally, the equivalent time delay must be less than 0.10 s.

Guidance for traditional stability margin requirements are given in MIL-F-87242[2] for all relevant modes, that is, those between 0.06 Hz and the frequency of the first aeroelastic mode. The gain and phase margin requirements for this design are ± 6.0 dB and ± 30 deg in all input and output loops. Because the longitudinal system has only a single input and multiple outputs, these classical robustness measures are considered acceptable for computing robustness at the input of the longitudinal system. Unfortunately, these gain and phase margins are not sufficient to ensure stability in the multivariable case, since small, simultaneous perturbations in several loops can destabilize a system, although individual loops may have sufficient gain and phase margins.

An alternative measure of robust stability is based on singular value techniques. Specifically, using structured singular value analysis, or μ analysis, to compute robustness to simultaneous perturbations in several loops gives a more reasonable measure of robustness for multivariable systems.[3,4] For the longitudinal control system, the structured singular value is computed for simultaneous perturbations in the loop gains at the sensor outputs. This gives a measure of the smallest destabilizing perturbation in each of the loop gains of the closed-loop system. For the lateral directional control system, the structured singular value is computed for

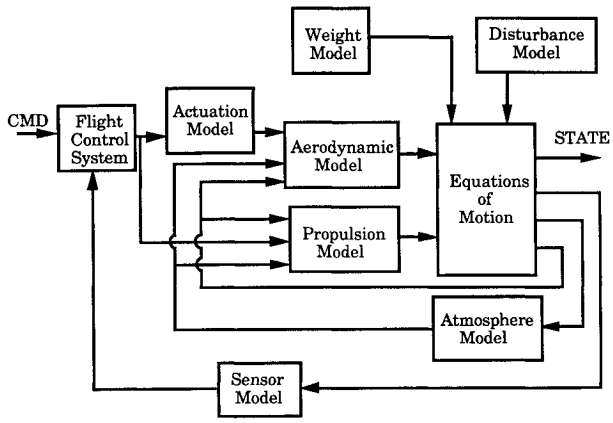

Fig. 1 VISTA nonlinear model structure.

simultaneous perturbations in the loop gains both at the actuator inputs and at the sensor outputs. Single-loop requirements do not translate to multivariable systems, since simultaneous perturbations are considered, and so the traditional 6-dB and 30-deg margins specifications cannot be used.

Aircraft Model

The VISTA F-16 aircraft is a lightweight, single engine, supersonic test vehicle. The aircraft is statically unstable in pitch for increased performance. The aircraft has leading- and trailing-edge flaps, an all moveable horizontal tail, and a single rudder. The horizontal tail is used symmetrically for pitch control and differentially for roll control. The pilot controls include a force-feel side stick, rudder pedals, and a throttle.

A high-fidelity, six-degree-of-freedom, nonlinear simulation model has been developed for the VISTA F-16 vehicle. The VISTA nonlinear model is written as a series of FORTRAN subroutines, and implemented and validated in a generic nonlinear simulation environment. Specific application modules include subroutines describing the equations of motion, actuators, and sensors. The actuation models for all of the control surface deflections include fourth-order linear dynamics, hinge moment effects, and position and rate limits. Additional subroutines describe the propulsion system, weight and moments of inertia variations, the atmosphere, and the existing digital fly-by-wire control system. The aerodynamic data exists for a wide range of Mach numbers, altitudes, and angles of attack and sideslip. The model is detailed enough to simulate long duration and large-amplitude maneuvers with extreme accuracy. The nonlinear model is used to generate linear models for control law design and to generate nonlinear time histories to evaluate control designs. A diagram of the VISTA F-16 nonlinear model structure is shown in Fig. 1, where CMD represents the pilot command.

Linear Model Description

Once a trim condition is established for the nonlinear aircraft model within the simulation environment, a linear model is generated to capture the perturbational dynamics around the equilibrium point. Linear models are generated for the open-loop aircraft using two-sided perturbations to evaluate the necessary partial differentials. Linear design models are generated at several different flight conditions corresponding to different Mach numbers and altitudes. Separate sets of linear design points were used for the design of the longitudinal and lateral directional flight control laws. The design flight conditions are shown in Figs. 2 and 3.

The linearization procedure yields a 10th-order model of open-loop aircraft dynamics. The model states are transformed into conventional aircraft states: Euler angles, body axis rotational rates, forward speed, angles of attack and sideslip, and altitude. For a wings level trimmed condition, the linear model consists of decoupled fifth-order longitudinal and lateral directional models. The longitudinal linear model is reduced to second order by removing the trajectory states: altitude, velocity, and pitch angle. This model reduction essentially removes the neutrally stable altitude mode and the phugoid mode, leaving the short period dynamics relatively unchanged. The remaining model reflects the aircraft dynamics in maneuvering flight,

$$\begin{aligned} \dot{\alpha} &= Z_\alpha \alpha + q + Z_{\delta e}\delta_e \\ \dot{q} &= M_\alpha \alpha + M_q q + M_{\delta e}\delta_e \\ A_z &= V(Z_\alpha \alpha + Z_{\delta e}\delta e) \end{aligned} \tag{4}$$

The lateral directional linear model is reduced to third order by removing the trajectory states: the neutrally stable heading angle and the roll angle. Removing the roll angle removes the neutrally stable spiral mode and leaves the roll and Dutch roll mode poles relatively unchanged. The lateral directional linear model becomes

$$\begin{aligned} \dot{\beta} &= Y_\beta \beta + \frac{W_0}{V} p - \frac{U_0}{V} r + Y_{\delta f}\delta_{df} + Y_{\delta dt}\delta_{dt} + Y_{\delta r}\delta_r \\ \dot{p} &= L_\beta \beta + L_p p + L_r r + L_{\delta f}\delta_{df} + L_{\delta dt}\delta_{dt} + L_{\delta r}\delta_r \\ \dot{r} &= N_\beta \beta + N_p p + N_r r + N_{\delta f}\delta_{df} + N_{\delta dt}\delta_{dt} + N_{\delta r}\delta_r \end{aligned} \tag{5}$$

The measured outputs are pitch, roll, and yaw rates; normal acceleration; angle of attack; and sideslip angle. It was assumed

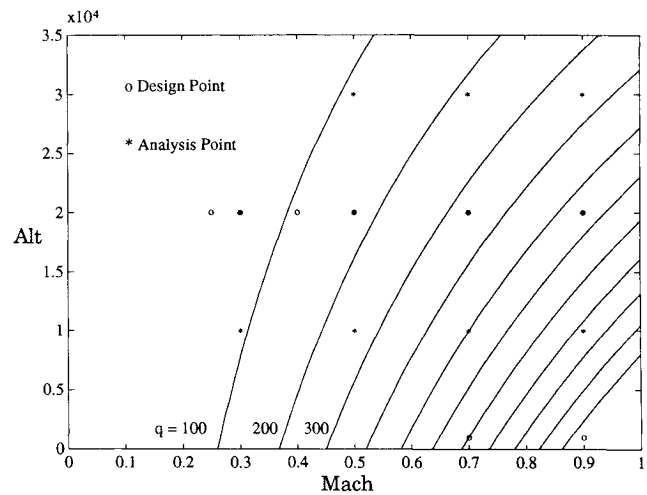

Fig. 2 Longitudinal design envelope.

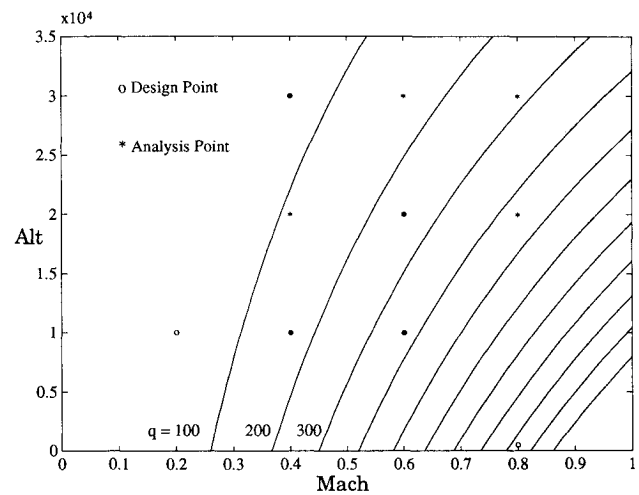

Fig. 3 Lateral/directional design envelope.

for this design that angle of attack and sideslip angle could either be measured directly or reconstructed from inertial data. Only one weight and store configuration and the trim throttle setting were used in the design and in the analysis. Stores consist of two AIM-9 missiles on the wingtips.

Control Law Design

Proportional plus integral output feedback controllers are designed separately for the longitudinal and lateral directional axis. Figures 4 and 5 show the structure of the flight control system. LQR theory is used to synthesize the feedback gains for both axes. Consider a linear, time-invariant model

$$\dot{x} = Ax + Bu \tag{6}$$

A quadratic performance index of the criterion outputs z is given by

$$J = \int_0^\infty z^T Q z \, dt \tag{7}$$

where

$$z = Fx + Gu \tag{8}$$

Here, the weighting matrix Q is used as a design variable to trade off different criterion outputs in the cost function. The criterion outputs are functions of the states and inputs of the linear plant model.

The state feedback control law is given by

$$u = -K_c x = -(G^T Q F + B^T P)x \tag{9}$$

where P is the stabilizing solution to the Riccati equation

$$(A - BG^T QF)^T P + P(A - BG^T QF) - PBB^T P + F^T(I - GG^T Q)^T Q(I - GG^T Q)F = 0 \tag{10}$$

Longitudinal Design

The VISTA F-16 is statically unstable in the pitch axis over most of the flight envelope. The longitudinal flight control system must provide inputs to the horizontal tail to stabilize the aircraft and provide satisfactory handling qualities. For this design study, the angle of attack, pitch rate, and normal acceleration sensor outputs are used to drive the longitudinal controller. To provide the required response to pilot stick inputs for a wide flight envelope, a dual command control structure is used. An angle-of-attack command system is employed at low-dynamic pressures and a normal acceleration command is used at high-dynamic pressures.[5] Integral feedback in the commanded variable produces good low-frequency tracking.

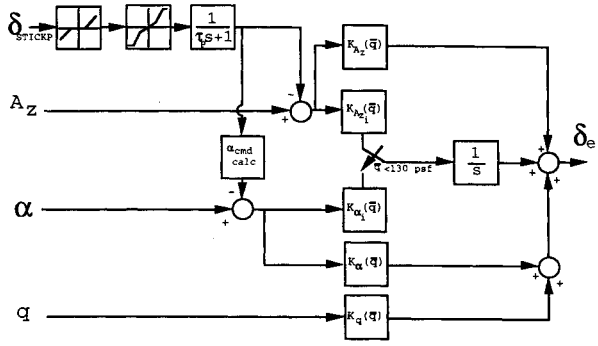

Fig. 4 Longitudinal control system.

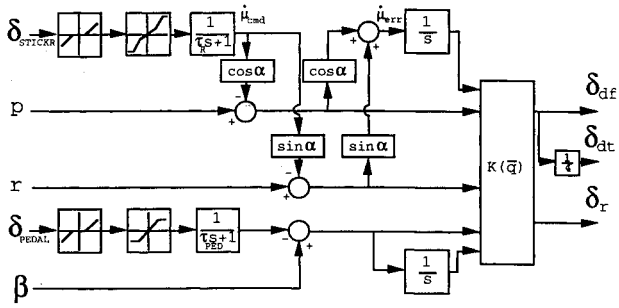

Fig. 5 Lateral/directional control system.

The open-loop longitudinal model is put into state-space form for control law design

$$\dot{x}_{\text{lon}} = A_{\text{lon}} x_{\text{lon}} + B_{\text{lon}} u_{\text{lon}} \tag{11}$$

$$x_{\text{lon}} = [\alpha \; q \; \int e \, dt]^T, \qquad u_{\text{lon}} = \delta_e \tag{12}$$

where x_{lon} and u_{lon} are the longitudinal state and control vectors. The signal e is the tracking error to a reference command r_c. For a normal acceleration command design, $e = A_z - r_c$, and for an angle-of-attack command design, $e = \alpha - r_c$.

The criterion outputs for longitudinal control synthesis are

$$z_1 = \alpha \qquad z_2 = q$$

$$z_3 = \int e \, dt \qquad z_4 = \delta_e \tag{13}$$

Initial selection of the weighting matrices is based on Bryson's rule[6]

$$Q_{ii} = 1/z_{i_{\max}}^2 \tag{14}$$

where Q_{ii} are the diagonal elements of the criterion output weighting matrix. The variables $z_{i_{\max}}$ are the maximum allowable values for each of the criterion outputs z_i. The weights are fine tuned to place the closed-loop poles at suitable locations for flying qualities.

In the longitudinal case, since normal acceleration, angle of attack, pitch rate, and integrated tracking error are available, the number of outputs exceeds the number of states in the design model. The output vector is

$$y_{\text{lon}} = C_{\text{lon}} x_{\text{lon}} + D_{\text{lon}} u_{\text{lon}} \tag{15}$$

Because the matrix C_{lon} has full column rank, an output feedback gain matrix can be derived that preserves the closed-loop eigenstructure. The state feedback equation can be rewritten as a function of C_{lon} and a diagonal matrix S.

$$u_{\text{lon}} = -K_{c_{\text{lon}}} x_{\text{lon}} = -K_{c_{\text{lon}}} (C_{\text{lon}}^T S C_{\text{lon}})^{-1} C_{\text{lon}}^T S C_{\text{lon}} x_{\text{lon}} \tag{16}$$

Using Eqs. (15) and (16), the feedback solution can be expressed in terms of the output y and the matrices C_{lon} and D_{lon}.

$$C_{\text{lon}} x_{\text{lon}} = y_{\text{lon}} - D_{\text{lon}} u_{\text{lon}} \tag{17}$$

$$u_{\text{lon}} = -K_{c_{\text{lon}}} (C_{\text{lon}}^T S C_{\text{lon}})^{-1} C_{\text{lon}}^T S (y_{\text{lon}} - D_{\text{lon}} u_{\text{lon}}) \tag{18}$$

$$u_{\text{lon}} = -[I - K_{c_{\text{lon}}} (C_{\text{lon}}^T S C_{\text{lon}})^{-1} C_{\text{lon}}^T S D_{\text{lon}}]^{-1} K_{c_{\text{lon}}} \times (C_{\text{lon}}^T S C_{\text{lon}})^{-1} C_{\text{lon}}^T S y = -K_{y_{\text{lon}}} y \tag{19}$$

The diagonal matrix S can be chosen to adjust the gains on particular feedback signals to reflect design considerations such as output response characteristics. It is important to note that because the output feedback system is not strictly proper, the state feedback stability margin guarantees are no longer valid. In this case, particular care must be taken in the selection of the output feedback transformation so that stability robustness properties are not destroyed.

Separate designs were completed for each of the eight design points shown in Fig. 2. The points chosen represent a range of

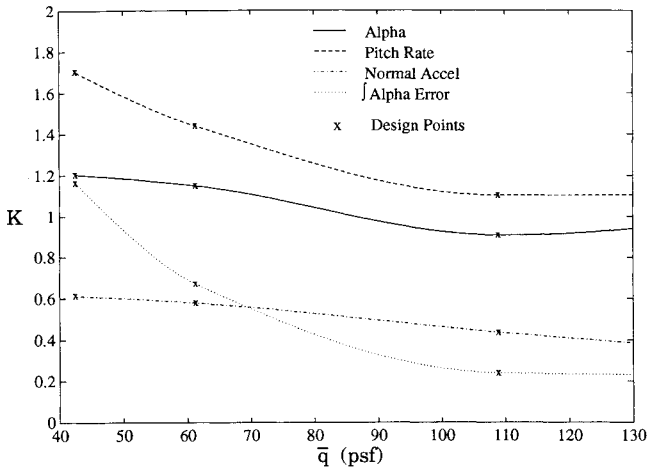

Fig. 6 Longitudinal gains for low $\bar{q}$.

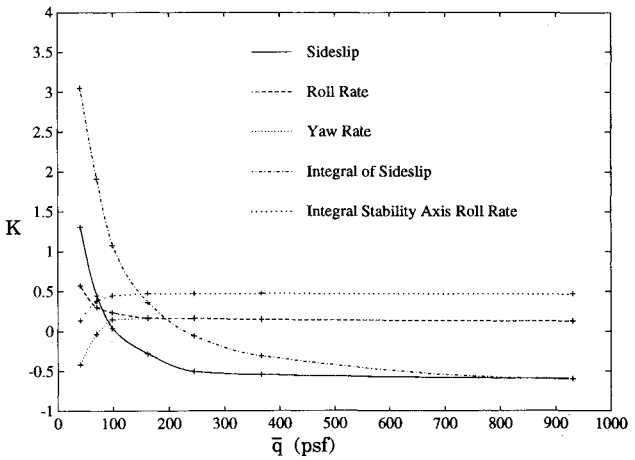

Fig. 8 Aileron gains.

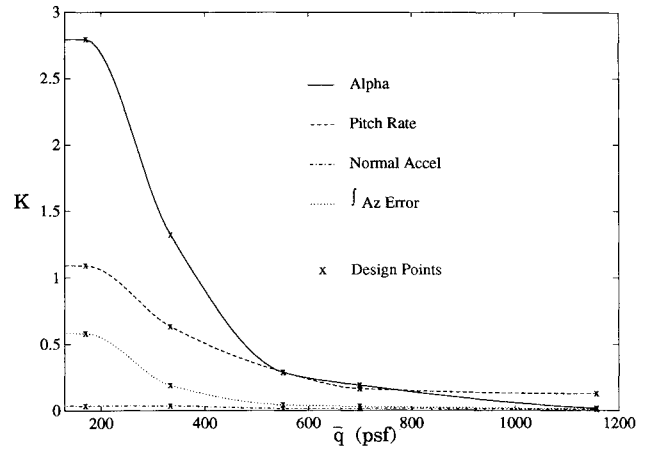

Fig. 7 Longitudinal gains for high $\bar{q}$.

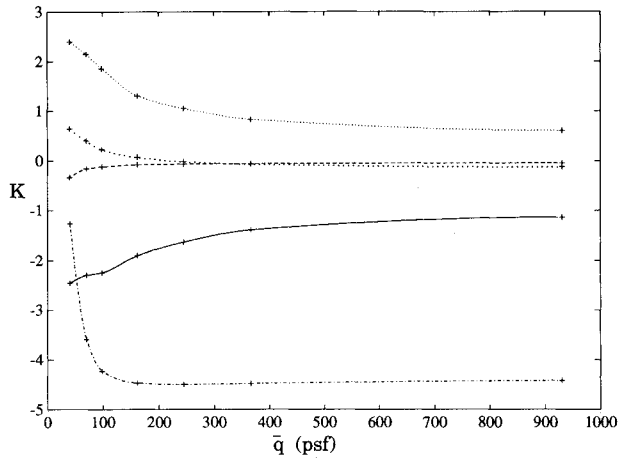

Fig. 9 Rudder gains.

dynamic pressures and angles of attack. For each point design, the design weights were adjusted to achieve the desired closed-loop flying qualities. For each point, there are three proportional gains and one integral gain.

Lateral Directional Design

The lateral directional flight control system must provide satisfactory handling qualities through control of stability axis roll rate and sideslip angle. Integrators on the stability axis roll rate and the sideslip angle signals provide good steady-state response. The two integrators result in two additional states. The resulting synthesis model has five states: sideslip angle, roll rate, yaw rate, integral of sideslip angle error, and integral of stability axis roll rate error. Since roll and yaw rates and sideslip angle are measured, and the integrated error signals are generated, all of the states of the linear model are available for feedback.

The inputs to the lateral directional dynamics are the differential horizontal tail, the differential flaperon, and the rudder. The deflections of the differential flaperon and the differential tail are combined to form a single input in the linear model (δ_a). This is done to represent the hardware of the actual vehicle. The combined control effectiveness of the flaperon and differential tail is formed by summing the control effectiveness of the flaperon and one-fourth that of the tail. Thus, a single input is created in the design model. In the implementation of the control laws, the command sent to the differential flaperon is scaled by one-fourth and sent to the differential tail.[7] The linear design model is

$$\dot{x}_{\text{lat}} = A_{\text{lat}} x_{\text{lat}} + B_{\text{lat}} u_{\text{lat}} \tag{20}$$

$$x_{\text{lat}} = [\beta_{\text{err}}\ p_{\text{err}}\ r_{\text{err}} \int \beta_{\text{err}}\, dt \int \dot{\mu}_{\text{err}}\, dt]^T, \qquad u_{\text{lat}} = [\delta_a\ \delta_r] \tag{21}$$

where x_{lat} and u_{lat} are the lateral directional state and control vectors. The stability axis roll rate signal is generated as a function of body axis roll, body axis yaw, and angle of attack

$$\mu_{\text{err}} = p_{\text{err}} \cos\alpha + r_{\text{err}} \sin\alpha \tag{22}$$

For the linear point designs, the values for the components of α in the stability axis roll rate signal were assumed to be constant. In the nonlinear implementation, the nonlinear elements are included in the feedback path between the angle of attack and the stability axis roll rate signal.

The criterion outputs were chosen to achieve good flying qualities in the closed-loop design. Combinations of states are created to produce zeros in the criterion outputs. The desired closed-loop poles are used to select the criterion outputs, since the closed-loop poles will approach these zeros. The desired flying qualities are used to select these zeros, providing a way to incorporate desired flying qualities into the design.[8]

For the lateral directional model in this design, the first criterion output is a combination of roll rate, yaw rate, and integrated stability axis roll rate error, and is given by

$$z_1 = \left(\frac{s + K_I}{s}\right)\dot{\mu}_{\text{err}}$$

$$= \dot{\mu}_{\text{err}} + K_I \int \dot{\mu}_{\text{err}}\, dt$$

$$= p_{\text{err}} \cos\alpha + r_{\text{err}} \sin\alpha + K_I \int \dot{\mu}_{\text{err}}\, dt \tag{23}$$

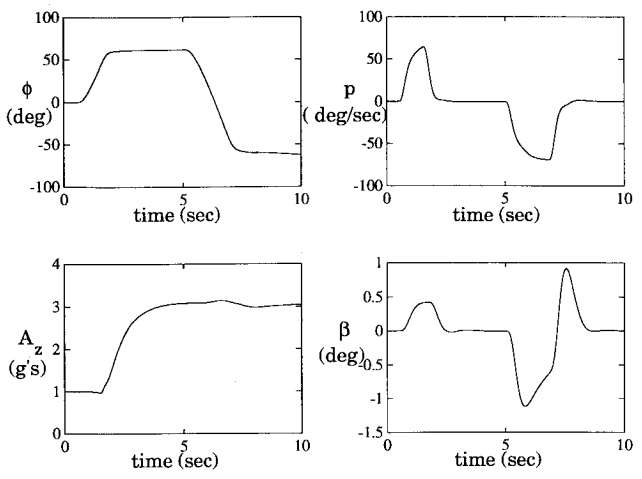

Fig. 10 Time history of loaded roll maneuver.

The second criterion output is a combination of sideslip angle, integrated sideslip angle, and the derivative of sideslip and is given by

$$z_2 = \left(\frac{s^2 + 2\zeta\omega s + \omega^2}{s}\right)\beta_{\text{err}}$$

$$= \dot{\beta}_{\text{err}} + 2\zeta\omega\beta_{\text{err}} + \omega^2\int\beta_{\text{err}}\,dt$$

$$= Y_\beta\beta_{\text{err}} + \frac{W_0}{V}p_{\text{err}} - \frac{U_0}{V}r_{\text{err}}$$

$$+ Y_{\delta a}\delta_a + Y_{\delta r}\delta_r + 2\zeta\omega\beta_{\text{err}} + \omega^2\int\beta_{\text{err}}\,dt \qquad (24)$$

The derivative of the sideslip angle is formed using the sideslip equation in Eq. (5). A sensor for the derivative of sideslip is not required for control. The third and fourth criteria outputs are the control inputs:

$$z_3 = \delta_a \qquad z_4 = \delta_r \qquad (25)$$

The constants in Eqs. (23) and (24) are selected to make the zeros of the controlled output equations the desired closed-loop poles. The constant K_I in z_1 is chosen to specify the roll mode time constant. Similarly, the constants ω and ζ in z_2 are chosen to specify the Dutch roll damping and frequency. The criterion output weighting matrix Q_{lat} is a diagonal matrix that is used to adjust the relative weights of the criteria outputs in the cost function.

Separate designs were completed for each of the design points shown in Fig. 3. As in the longitudinal case, the points represent a range of dynamic pressures and angles of attack. The resulting feedback gain matrices have 10 elements, since there are five feedback signals and two independent inputs.

Nonlinear Implementation

The control law design covers the subsonic flight envelope for dynamic pressures between 40 and 1150 psf. Feedback gains are scheduled with dynamic pressure to establish a full envelope control law. Design points were selected at various altitudes and Mach numbers to capture a broad range of dynamic pressures. Figures 2 and 3 show the design points used in formulating the gain schedules. The gains at the linear design points are connected through a hermite cubic interpolation routine.[9] The interpolation routine is written in FORTRAN 77 and contained within the controller subroutine, thus creating a nonlinear control law implementation. The feedback gains for two longitudinal modes are plotted in Figs. 6 and 7. The lateral directional feedback gains are shown in Figs. 8 and 9. The gains shown are in units of deg/deg, deg/(deg/s), and deg/n.

Two different longitudinal gain schedules exist, one for the angle-of-attack mode and one for the normal acceleration command mode. The transition between the modes is controlled by a local trimming routine that ensures that there are no discontinuities in the actuator command at the time of transition. For dynamic pressures less than 130 psf, longitudinal stick inputs translate into angle-of-attack commands. For greater dynamic pressures a normal acceleration command is generated. Lateral stick inputs translate into roll rate commands, and rudder pedal inputs translate into sideslip angle commands.

First-order lag prefilters are used to smooth commands so that abrupt pilot inputs do not create abrupt aircraft responses. The longitudinal stick prefilter time constant is scheduled with dynamic pressure. The rudder prefilter time constant is fixed at 0.067 s. The roll rate prefilter has a variable time constant. For large commands the prefilter has a time constant of 0.4 s, and for small commands and for commands moving toward zero roll rate, the prefilter has a smaller time constant of 0.2 s. This allows the pilot to perform small maneuvers and to stop rolling crisply when the desired roll attitude is reached. Local feedback loops around the three integrators are closed in the event of control surface saturations. These conditional loops provide antiwindup protection to the control sys-

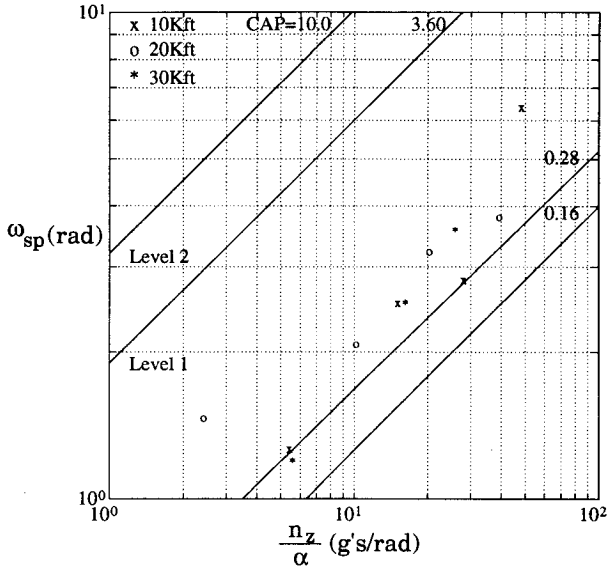

Fig. 11 Short period frequency results.

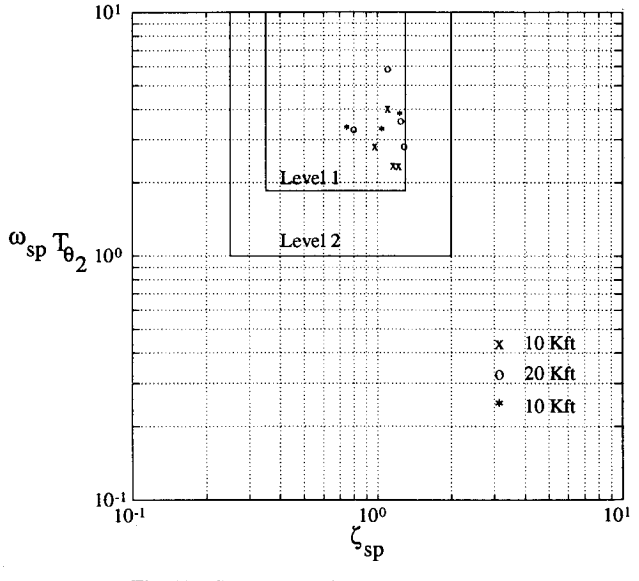

Fig. 12 Short term pitch response results.

tem during demanding maneuvers that may create unmanageable transient errors.

Figures 4 and 5 show that several nonlinear elements are included in the forward path of the control system. Deadbands in the stick and rudder pedal paths create command breakout forces that prevent small force disturbances from creating undesirable control action. Force gradients translate pilot stick and rudder pedal inputs into commands to the control system. Piecewise linear control gradients provide fine tracking capability for small stick inputs and gross maneuvering capability for large stick inputs. Linear first-order lag prefilters smooth the scaled pilot commands before they are used to generate the error signals in the control system.

The control laws were implemented in FORTRAN and used in the nonlinear simulation. The time history for a loaded roll maneuver starting at 20,000 ft, Mach 0.7 is shown in Fig. 10. A simulated pilot command is given to roll the aircraft to 60 deg, and then to command 3 g normal acceleration. The roll command is reversed, and the aircraft rolls from 60 deg to past 60 deg in the opposite direction. Both roll rate and normal acceleration are tracked very well. In particular, the load factor commanded is held very close to the commanded value during the loaded roll. Sideslip is regulated within ± 1.2 deg during the maneuver, showing that the coupled maneuver is well coordinated.

Flying Qualities Results

The closed-loop aircraft was evaluated at several points to quantify the flying quality parameters across the flight envelope. Figures 2 and 3 show the points that were used in the flying qualities analysis. The analysis points are a combination of design points and off design points. For the latter case, the gains were derived from the schedules in Figs. 6–9, and the linear aircraft models were obtained by linearizing the nonlinear model at the appropriate point. Both design and off design points were used in the analysis to assure good transition between flight conditions and good performance across the flight envelope.

Longitudinal

For each evaluation point shown in Fig. 2, an equivalent system transfer function matching program was used to match the high-order transfer function from pilot stick inputs to outputs of interest to the low-order equivalent systems in Eq. (1) over the frequency range between 0.1 and 10 rad/s. The second-order longitudinal dynamics, high-order actuator models, and the compensator were used to generate the high-order transfer function. Figure 11 shows that the short period natural frequency is greater than 1.0 rad/s for all conditions. The boundaries in Fig. 11 represent acceptable ranges for CAP. The level I boundaries are the middle lines. The

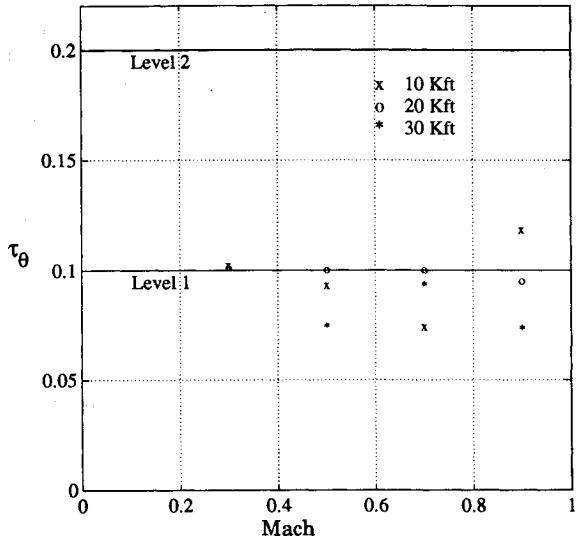

Fig. 13 Equivalent pitch time delay results.

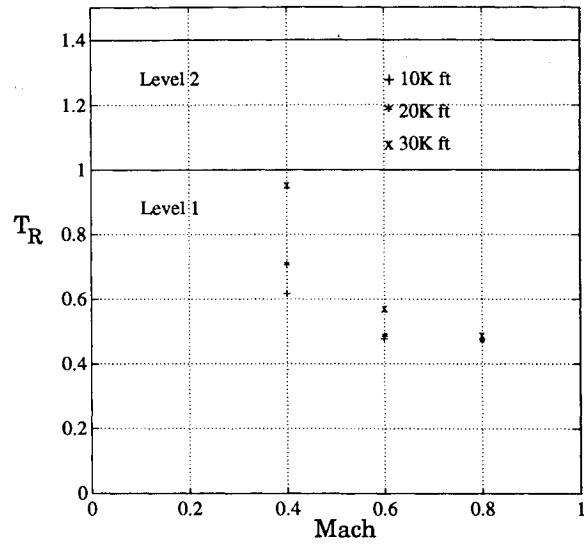

Fig. 15 Roll mode time constant results.

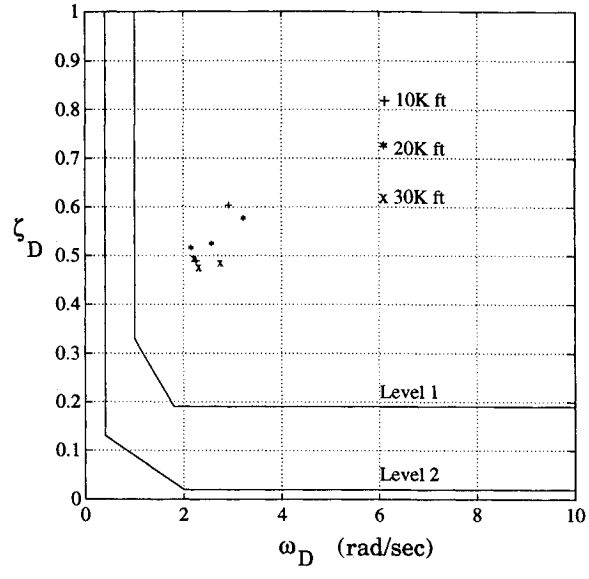

Fig. 14 Dutch roll frequency and damping results.

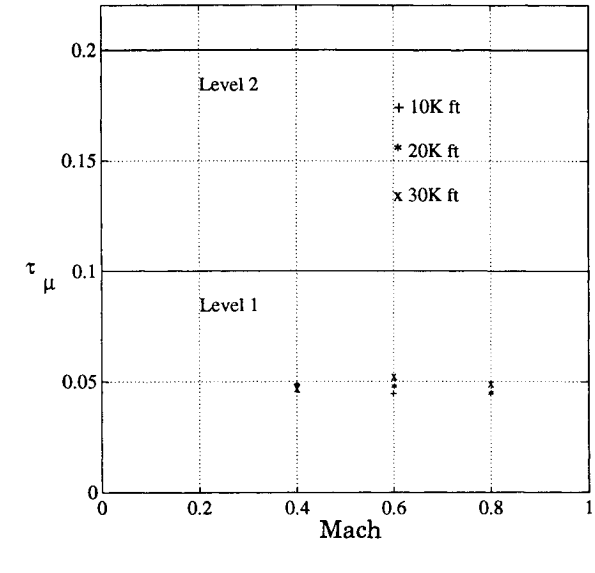

Fig. 16 Equivalent roll time delay results.

value of the control anticipation parameter falls slightly below the level I requirements at 30,000 ft and Mach 0.5.

Figure 12 shows that the short period damping and the product $\omega_{sp}T_{\theta 2}$ are level I for all conditions. As shown in Fig. 13, the equivalent pitch time delay requirement is the most difficult metric to satisfy. For Mach 0.3 and 10,000 ft and 20,000 ft, level I equivalent pitch time delay requirements are violated by 0.002 and 0.001 s, respectively. For Mach 0.9 and 10,000 ft, the equivalent time delay is 0.118 s. The excessive equivalent time delay at this condition is caused by coupling between the short period and actuator modes.

Lateral/Directional

The equivalent system transfer function matching program was used to fit the lateral stick force to stability axis roll rate transfer function to a third-order equivalent transfer function which includes the roll and Dutch roll modes. The fourth-order lateral directional dynamics, high-order actuator models, and the compensator were used to generate the high-order transfer function. The equivalent systems were matched for the frequency range between 0.1 and 10 rad/s. The Dutch roll frequency and damping, roll mode time constant, and equivalent roll time delay are plotted in Figs. 14–16. For each of the flight conditions where the flying qualities were tested, the values are well within the level I boundaries. The spiral stability was assessed from the high-order transfer function. At each of the design points the spiral mode was nearly neutrally stable. A spiral mode with level I flying qualities has a time to double amplitude after a disturbance in roll of at least 12 s. Thus, this requirement is met for all of the flight conditions.

Stability Margin Analysis

Gain and phase margins were computed at the input of the longitudinal plant for a wide array of flight conditions. The conditions tested were at 10*K*, 20*K*, and 30*K* ft altitude, and Mach numbers 0.3, 0.5, 0.7, and 0.9. Longitudinal input gain and phase margins exceed specifications for all test points.

Robustness at the output of the longitudinal system was computed by assuming each sensor loop had an independent, multiplicative perturbation bounded by unity magnitude. Each perturbation was allowed to vary independently in gain and phase, and the structured singular value was computed to obtain the magnitude of the smallest destabilizing perturbation. For the conditions tested, the structured singular values peak between 1.1 and 1.8 in the frequency range of the short period dynamics. The inverse of the peak values is the size of the smallest perturbation that makes a mode of the system, in this case the short period, unstable. Since this measure of robustness considers simultaneous, independent perturbations in gain and phase in each loop, the robustness is considered satisfactory.

Robustness at the input and output of the lateral directional system was computed in a similar fashion. The flight conditions tested were at 10*K*, 20*K*, and 30*K* ft altitude, and Mach numbers 0.4, 0.6, and 0.8. Simultaneous, independent perturbations were assumed first in the actuator loops and then in the sensor loops. The structured singular values for input perturbations are all less than unity, whereas the peak values for output perturbations are all in the range 1.7–2.3. This robustness is considered satisfactory.

Conclusions

A full envelope control system for both the longitudinal and lateral directional axes of the VISTA F-16 test aircraft has been developed. Linear quadratic synthesis provides state feedback solutions that are transformed into output feedback controllers with integral error states. A nonlinear control law has been created by scheduling feedback gains with dynamic pressure. The resulting flight control system has been implemented and tested within a high-fidelity, six-degree-of-freedom nonlinear simulation. Analysis demonstrates that the controller provides stability, robustness, and flying qualities for a broad range of flight conditions.

References

[1]"Military Specification—Flying Qualities of Piloted Vehicles," MIL-STD-1797, March 1987.

[2]"Military Specification—General Specification for Flight Control Systems," MIL-F-87242, March 1986.

[3]Dailey, R. L., "Lecture Notes for the Workshop on H_∞ and μ Methods for Robust Control," American Control Conference, San Diego, CA, May 1990.

[4]Doyle, J. C., "Analysis of Feedback Systems with Structured Uncertainties," *IEEE Proceedings*, Vol. 129, Pt. D, No. 6, 1982, pp. 242–250.

[5]Adams, R. J., Sparks, A. G., and Banda, S. S., "A Gain Scheduled Multivariable Design for a Manual Flight Control System," *Proceedings of the 1992 IEEE Conference on Control Applications* (Dayton, OH), Inst. of Electrical and Electronics Engineers, Piscataway, NJ, 1992, pp. 584–589.

[6]Bryson, A. E., and Ho, Y. C., *Applied Optimal Control*, Hemisphere, Washington, DC, 1975.

[7]Sparks, A. G., Adams, R. J., and Banda, S. S., "Multivariable Control of the Lateral Axis of a Fighter Aircraft," *Proceedings of the AIAA Guidance, Navigation, and Control Conference* (Hilton Head, SC), AIAA, Washington, DC, 1992, pp. 506–516 (AIAA Paper 92-4408).

[8]Thompson, C. M., Coleman, E. E., and Blight, J. D., "Integral LQG Controller Design for a Fighter Aircraft," *Proceedings of the AIAA Guidance, Navigation, and Control Conference* (Monterey, CA), AIAA, New York, 1987, pp. 866–895 (AIAA Paper 87-2452).

[9]Kahaner, K., Moler, C., and Nash, S., *Numerical Methods and Software*, Prentice-Hall, Englewood Cliffs, NJ, 1989, pp. 102–108.